Developing Normalized Crack Growth Curves for Tracking Damage in Aircraft

J. P. Gallagher* and H. D. Stalnaker†
Air Force Flight Dynamics Laboratory, Wright-Patterson Air Force Base, Ohio

This paper directs attention to the interrelationship between crack growth rate equations and the Normalized Crack Growth (NCG) curve concept used in the F-4 fighter damage tracking program. Crack growth rate equations, based on linear elastic fracture mechanics assumptions, provide the capability for predicting the influences of geometrical changes or of stress scaling. For the crack growth rate equations that describe the flight-by-flight generated data presented herein, generalized integral (or inverted) formulas are suggested that provide the rationale for developing NCG curves. Subject to the limitations described within the body of the paper, the NCG curve invariance assumption for tracking damage at different locations in an aircraft appears reasonable.

Introduction

In recent years, the Air Force has evolved a design philosophy[1] which assumes that cracks are initially present in all airframe Safety-of-Flight Structure.‡ The cracks assumed therein are those that would escape detection during NDI-type inspections with a specified frequency. A crack of given observable size represents a definite level of damage. Normally, however, the assumed initial cracks represent a level of damage that must grow substantially before reaching the critical levels required for loss of aircraft. The Air Force has accepted (for safety's sake) the philosophy that damage can be specified in terms of crack length and that the damage accumulation rate depends directly on the rate at which these assumed cracks grow. Aircraft (damage) tracking programs are now being developed on the basis of this crack-damage rate concept. Tracking programs are initiated primarily to identify differences in vehicle damage resulting from difference in input loading (design loads vs service loads, individual to individual vehicle loads, etc.). Tracking crack growth damage requires utilizing many of the techniques presently employed in fatigue crack initiation damage tracking programs.

This paper identifies a new feature contained in the F-4 fighter crack growth damage tracking program, the Normalized Crack Growth (NCG) curve concept.[3] This paper establishes the framework for deriving NCG curves by introducing the interrelationship between crack growth data reduction techniques[4] and life prediction. The application of the NCG curve concept is illustrated utilizing experimental flight-by-flight crack growth data. The information on basic crack growth data, on data reduction techniques and on crack growth rate equations is presented first. In the second half of the paper, the previously developed crack growth rate equations are utilized to formulate a rational basis for the NCG curve concept. Subsequent to the development of this framework for constructing NCG curves based on experimental crack growth rate results, a cost-effective method is introduced for generating crack growth rate results analytically.

Presented at the AIAA/ASME/SAE 17th Structures, Structural Dynamics, and Materials Conference, King of Prussia, Pa., May 5-7, 1976 (in bound volume of Conference papers, no preprint number); submitted June 7, 1976; revision received Nov. 28, 1977.

Index categories: Structural Design (including Loads); Safety; Reliability, Maintainability, and Logistics Support.

*Aerospace Engineer, Structural Integrity Branch.

†Aerospace Engineer, Experimental Branch. Member AIAA.

‡Safety-of-Flight Structure is defined in MIL-A-83444[2] to be: That structure whose failure could cause direct loss of the aircraft, or whose failure, if it remained undetected, could result in loss of the aircraft.

Crack Growth Rate Formulation

Spectrum and Crack Growth Data

The flight-by-flight history utilized in this investigation was the 135,000-cycles-per-lifetime bomber design stress history studied by Potter.[5] The sequence stress history was composed of three missions, herein designated as **A**, **B**, and **C**, and was applied in repeating blocks of 100 flights arranged accordingly:

$$9\times[9\times\mathbf{A}+\mathbf{B}]+[9\times\mathbf{A}+\mathbf{C}]$$

The missions **B** and **C** contained **A** mission load events and those additional (nonfrequent) load events required to match the design exceedance curve. Stress level scaling factors were applied to give three stress histories with maximum spectrum stresses of 24.17, 31.17, and 36.31 ksi. These stress histories were applied to nominally ½-in.-thick, 6.0-in.-wide 7075-T651 aluminum specimens containing two parallel, centrally located, through-thickness cracks, as illustrated in Fig. 1. Crack growth was visually monitored using binocular zoom microscopes with a maximum magnification of 40×. Crack length readings were estimated to be accurate within ±0.002 in. (±0.001 in. for short cracks). The applied loads were maintained to within 3% of the required values. Figure 2 summarizes the crack growth behavior observed in each of three test specimens (two cracks per specimen). The crack growth behavior is typically expressed as crack length as a function of life expended, in this case flights. Each specimen was subjected to the same stress sequence but the stress levels were scaled to the level identified.

Crack Growth Rate Data

Figure 3 provides a crack growth rate description of the data shown in Fig. 2 for the crack length intervals defined by Table 1. As can be seen from Fig. 3, the dispersion in the growth rate data is small and the mean behavior increases as a function of a characteristic stress intensity factor.§ The flight-

§$K_{max}=(K/\sigma)\sigma_{max}$

where

σ_{max} = maximum stress in stress history
K/σ = $\beta\sqrt{\pi a}$ = stress intensity factor coefficient
β = $1.0+0.2565\,(a/W)-1.152\,(a/W)^2+12.20\,(a/W)^3$

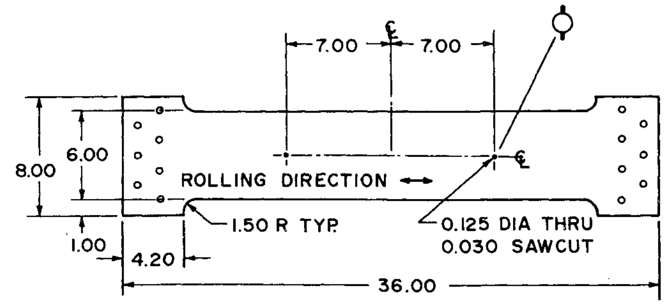

Fig. 1 Specimen geometry.

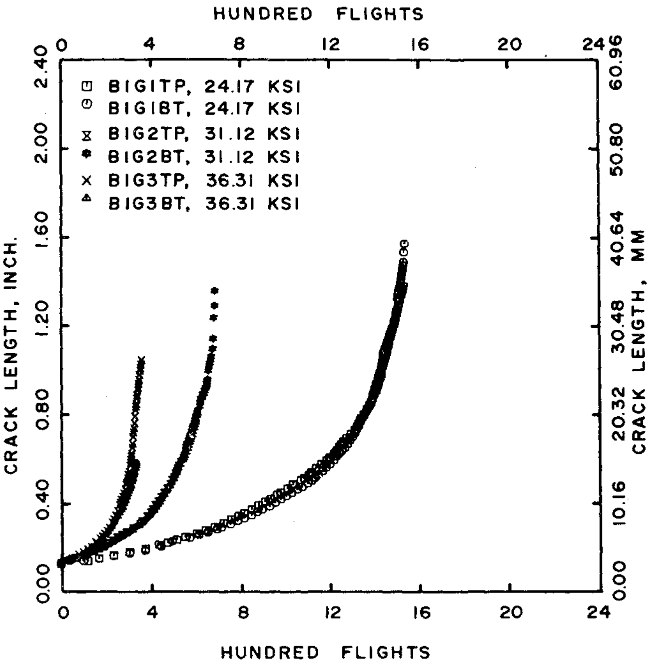

Fig. 2 Experimental flight-by-flight fatigue crack growth behavior (three stress levels considered).

by-flight crack growth rate behavior illustrated in Fig. 3 meets the conditions in general for steady-state crack growth rate behavior,[6] i.e., behavior similar to that exhibited under typical constant amplitude input conditions. The crack growth rate data presented in Fig. 3 were generated using the scheme outlined in Fig. 4 through step d.

Selecting the Growth Rate Equation

The paper is concerned with applying crack growth rate equations of the form

$$\frac{da}{dF}=C_I\,(K_{max})^{p_I} \tag{1}$$

and

$$\frac{da}{dF}=\frac{C(K_{max})^{p}}{K_c-K_{max}} \tag{2}$$

to the data shown in Fig. 3. Equations such as Eqs. (1) and (2) have previously been found suitable for describing the central region of constant-amplitude fatigue crack growth rate data.[4,6] Determination of the most appropriate equation will be established by applying steps e and f of Fig. 4. The most appropriate equation is expected to 1) describe the trend and magnitude of the crack growth rate behavior, and 2) repredict in integral form the original crack growth data. To sense the ability of a least-squares-derived equation for describing the crack growth rate data, two statistical measures were used. The coefficient of correlation R provided the measure that determined closeness of fit, and the modified standard error M was used to measure data dispersion about the curve. Equations (3) and (4) define these two measures:

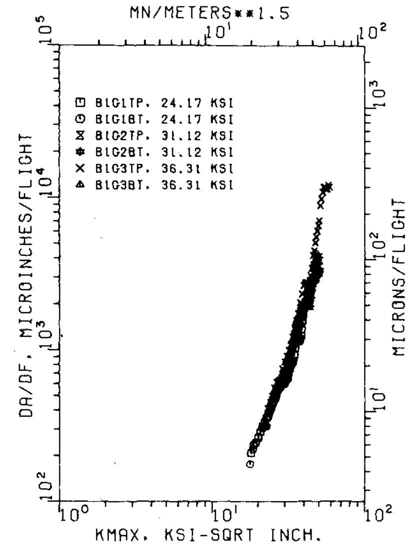

Fig. 3 Flight-by-flight induced crack growth rate behavior described as a function of stress intensity factor.

$$R=\left[\sum_{j=1}^{Z}(Y_{est}-\bar{Y})^2\Big/\sum_{j=1}^{Z}(Y-\bar{Y})^2\right]^{1/2} \tag{3}$$

and

$$M=\left[\sum_{j=1}^{Z}(Y-Y_{est})^2\Big/(Z-2)\right]^{1/2} \tag{4}$$

where Z is the number of crack growth rate data points and the Y's are logarithmic values of the crack growth rate, i.e.

$$Y=\ln\left(\frac{da}{dF}\Big|_j\right)\quad j\text{th data point} \tag{5a}$$

$$Y_{est}=\ln\left(\frac{da}{dF}\right)\quad \frac{da}{dF}\text{ from Eqs. (1) or (2) for a given }K_{max_j} \tag{5b}$$

$$\bar{Y}=\sum_{j=1}^{Z}(Y/Z) \tag{5c}$$

To determine the accuracy associated with the integrated form of the growth rate equation, the number of flights (predicted) required to grow the crack through the interval

Table 1 Limits on crack growth intervals for crack growth rate study

Crack designation	Max. stress level (σ_{max}), ksi	Initial crack length (a_0), in.	Final crack length (a_f), in.	Flights to propagate (N_f)
BIG1TP	24.17	0.133	0.834	1363
BIG1BT		0.133	0.845	1371
BIG2TP	31.12	0.134	0.820	613
BIG2BT		0.134	0.823	610
BIG3TP	36.31	0.130	0.839	333
BIG3BT		0.133	0.588	338

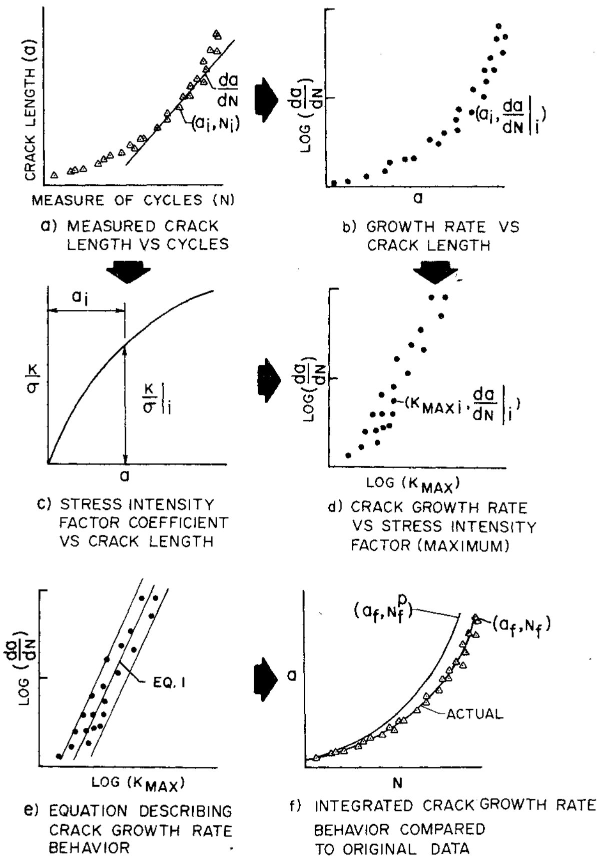

Fig. 4 Schematic of steps associated with establishing and validating a crack growth rate equation

defined by Table 1 was compared to the experimentally determined levels. The integral forms of Eqs. (1) and (2) for the crack length interval $a_0 < a_i \leq a_f$ are given by

$$N_i^p = \int_{a_0}^{a_i} \frac{\mathrm{d}a}{C_I (K_{\max})^{p_I}} \tag{6}$$

and

$$N_i^p = \int_{a_0}^{a_i} \frac{(K_c - K_{\max})\,\mathrm{d}a}{C(K_{\max})^{p}} \tag{7}$$

Table 2 Constants and evaluation for individual data sets

Crack designation	$C_I \times 10^7$	p_I	R	M	N_f^p/N_f
BIG1TP	0.878	2.65	0.983	0.114	1.004
BIG1BT					1.003
BIG2TP	0.405	2.91	0.988	0.102	1.023
BIG2BT					1.034
BIG3TP	0.0072	4.07	0.980	0.173	1.176
BIG3BT					1.033

Table 3 Constants for Eqs. (1) and (2)

Eq. no.	K_c, ksi$\sqrt{\text{in.}}$	C_I or C^a	p_I or p	R	M
(1)	...	0.1122×10^{-7}	3.28	0.971	0.214
(2)	70	1.64×10^{-5}	2.21	0.977	0.172
(2)	75	1.11×10^{-5}	2.36	0.974	0.178
(2)	80	0.84×10^{-5}	2.48	0.973	0.183

[a] Units of ksi$\sqrt{\text{in.}}$ and in./flight used to establish C_I and C.

respectively. N_i^p is used in Eqs. (6) and (7) as the generic term for fatigue life (predicted) to the crack length a_i. Once a crack growth rate expression like either Eq. (1) or (2) is developed, the principles of linear elastic fracture mechanics are assumed to apply.[7,8] On this basis, the constants in Eqs. (6) and (7) are assumed to be independent of crack length, geometry, or stress level changes since the model builds in the effect of these changes via the stress intensity factor.

Selection of a crack growth rate equation normally proceeds by iterative application of the scheme outlined in Fig. 4 where first one, then two, and then other groupings of multiple data input sets are analyzed, reduced to growth rate format, and repredicted; thus, anomalies in any data set might be easily identified by direct comparison to the other data sets and, thereafter, be excluded from further consideration. During the evaluation of Eq. (1), for example, the data subsets identified in Fig. 5 were considered. Table 2 provides a listing of the least-squares-determined constants (C_I and p_I) along with the measures of equation accuracy identified above.

Tables 3 and 4 provide the parameters associated with evaluation of Eqs. (1) and (2) to the data shown in Fig. 3. The equation (with associated coefficients) that results in the highest R, the lowest M, and life-prediction ratios that closely

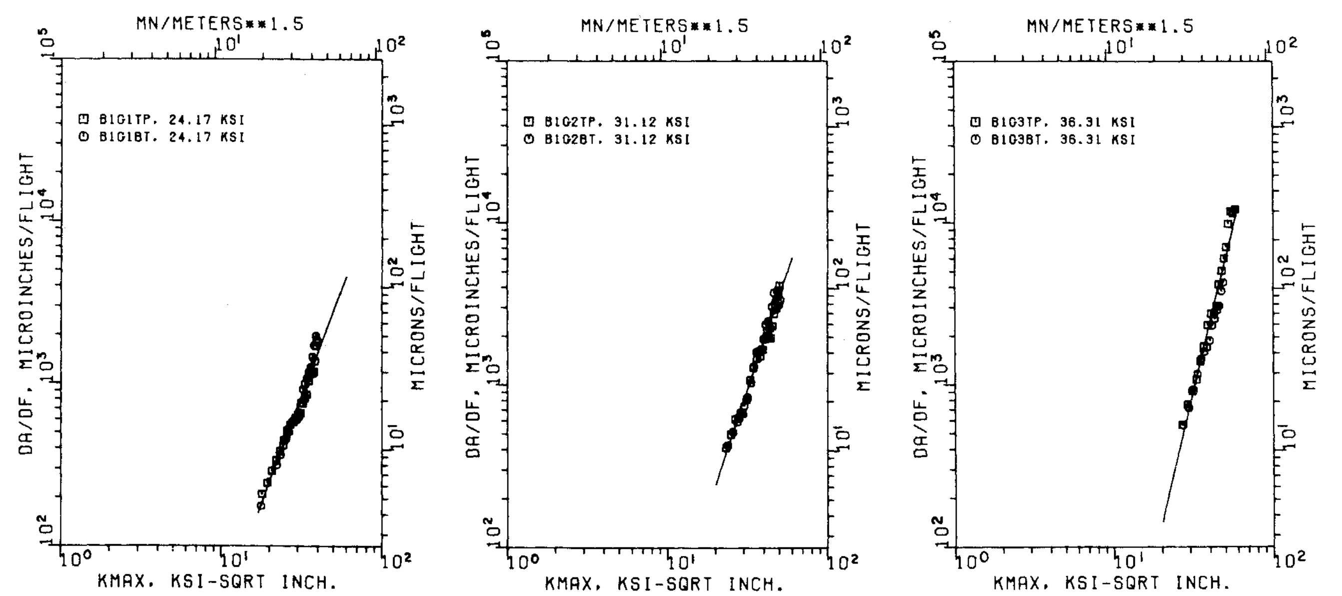

Fig. 5 Crack growth rate behavior of each test considered separately.

Table 4 Life prediction comparison between Eqs. (1) and (2)

Crack	Eq. (1)	Eq. (2) with K_c [a] of 70	75	80
BIG1TP	1.080	0.959	0.981	0.997
BIG1BT	1.086	0.956	0.985	1.001
BIG2TP	1.034	1.023	1.024	1.026
BIG2BT	1.054	1.040	1.043	1.045
BIG3TP	1.202	1.189	1.192	1.194
BIG3BT	1.036	1.058	1.054	1.051
Average	1.082	1.038	1.047	1.053

[a] Units of ksi $\sqrt{\text{in}}$.

scatter about 1.0 is considered the most appropriate (in the considered set) for describing these crack growth rate data. Based on the accuracy evaluation given in Tables 3 and 4, Eq. (2) as expressed in Eq. (8) was selected as the most appropriate equation:

$$\frac{da}{dF} = \frac{1.64 \times 10^{-5} K_{\max}^{2.21}}{70 - K_{\max}} \tag{8}$$

Equation (8) is directly compared to the crack growth rate in Fig. 6. In Fig. 7, the integral form of Eq. (8), i.e., Eq. (7), is successfully compared to the original crack growth data first presented in Fig. 2.

Now that crack growth rate formulations are available, the discussion will center on the application of such formulations to the development of tracking program concepts.

Normalized Crack Growth (NCG) Curve Concept

Background

When the crack growth behavior associated with the different structurally critical locations of the F-4 were examined by a team of McDonnell and Air Force engineers, it was noted that normalizing the crack growth curves to the forms illustrated in Fig. 8 provided a strong indication of similar behavior among locations in the airframe.[3,9] For both formats illustrated (Type I and Type II), the crack growth behavior (or damage) is described as a function of the fractional life required to extend the crack between the initial and final crack lengths (a_0 and a_f). The Type I format describes a life normalization scheme in which the ordinate expresses the crack size (a_i), between the specified initial size (a_0) and the final size (a_f), and the abscissa expresses the percent of total life expended in growing the crack to a_i. The Type II format presents a second normalized life scheme in which the ordinate is nondimensionalized to express the percent of growth from the initial crack size to the final crack length.

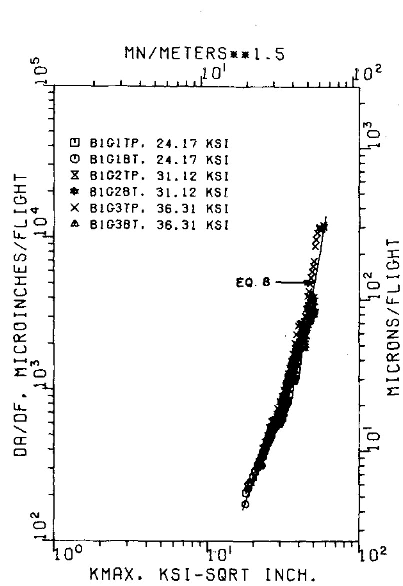

Fig. 6 Crack growth rate described using Eq. (8).

The principal difference between the two formats is due to the choices of initial and final crack lengths. The specific uses of the NCG curves as they are used to track crack growth damage in F-4 aircraft help to clarify the differences.

The Type I format is used when scheduling modifications and structural repair. For this format, both a_0 and a_f are constant; a_0 is set by an initial crack condition that could be expected to occur at a frequency approaching once per air-

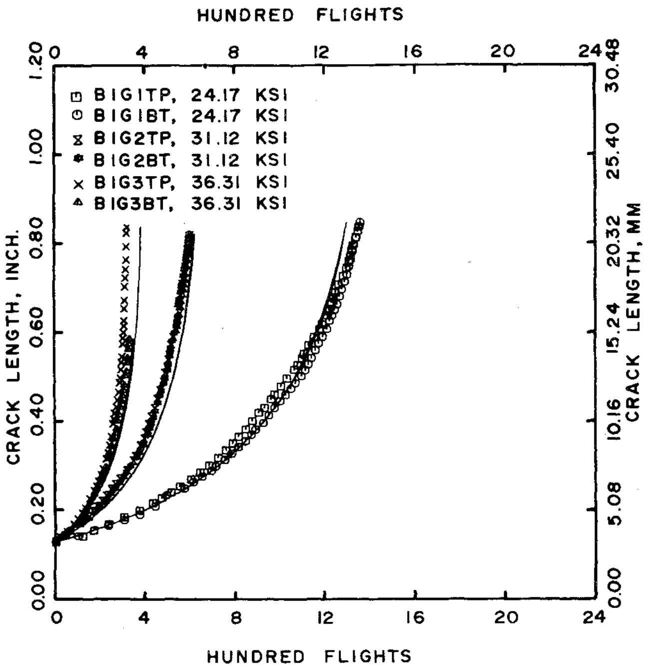

Fig. 7 Integrated version of Eq. (8) compared to original crack growth behavior from Fig. 2.

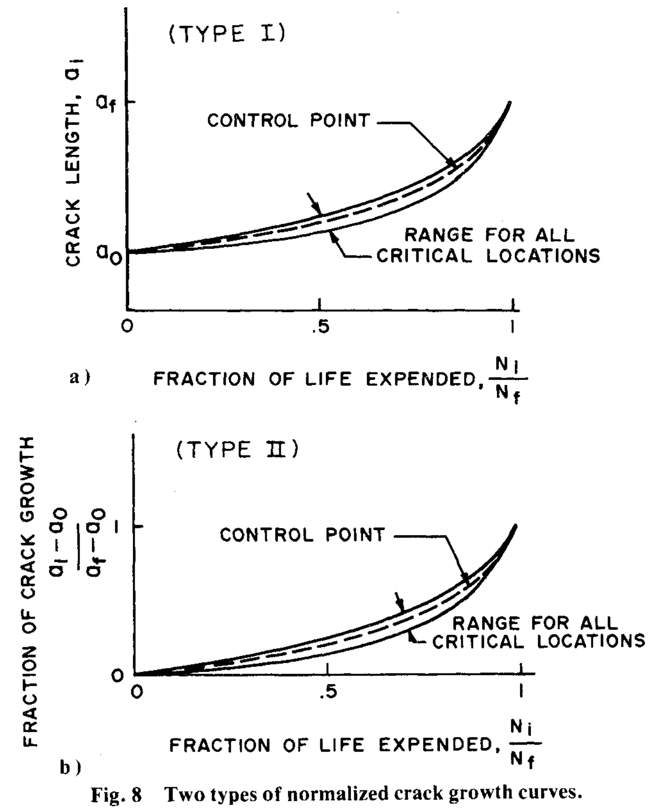

Fig. 8 Two types of normalized crack growth curves.

craft; a_f is the largest crack that can be safely removed by the repair process. The initial crack length (a_0) was established by variability studies of average aircraft quality such as those reported by Pinckert[9] and by Rudd and Gray.[10] The final crack size (a_f) was established as the crack length that would be removed through the reworking operation, e.g., by a hole-over-sizing-repair procedure. For a given type of cracking problem, say a hole cracking problem, fixing a_0 and a_f can have the advantage of removing geometrical influences from crack growth damage calculations, as well as making it possible to translate calculated or measured damage between locations on an individual aircraft.

The Type II format was used exclusively to establish inspection schedules and fracture critical (time) limits past which the cracking problem would impair aircraft safety. In the Type II NCG curve, only a_0 is constant, while a_f is a variable that depends on fracture toughness, part geometry, crack geometry, and the maximum service stress expected at the locations for which the curve is defined. For safety (fracture) critical parts, the initial crack size (a_0) was selected as the "worst possible" initial crack that could exist in any aircraft in the complete F-4 force; alternately, a_0 could have been established by the MIL-A-83444[2] requirements. The final crack size was established for each fracture critical location in the F-4 force using linear elastic fracture mechanics calculations, full-scale durability test article cracking data, and service experience cracking data.

Using the NCG procedure and considering the critical area selected as the control or monitoring point, less than 10% variation would be expected in the predictions of either inspection or modification times for an individual F-4 aircraft. It was concluded from the F-4 study that the crack growth behavior for any single control point could be monitored and the crack growth at all locations of interest could be determined. Additional information on the application of NCG curves in the F-4 tracking program can be found in Refs. 3 and 9.

Invariance of the NCG Curve

Based on the F-4 fighter study, the Type I and Type II NCG curves were identified to represent the materials response during cracking in a given structural configuration. The shapes that these response curves assumed were, for the most part, shown to be invariant with respect to external inputs (stress history). By direct implication, crack growth lives for specified geometries are a separable function of identifiable geometry and stress inputs. When the maximum stress intensity factor (K_{max}) in Eqs. (6) and (7) is replaced with its equivalent, $\sigma_{max}\beta\sqrt{\pi a}$, the equations can each be rewritten in an attempt to separate stress and geometrical components. The attempt was partially successful as indicated by the bracketed terms in Eq. (9) [equivalent to Eq. (6)]; however, the stress and geometric effects are noted to be coupled for the Eq. (7) case (not written).

$$N_i^p = \left[\frac{1}{C_I(\sigma_{max})^{p_I}}\right]\cdot\left[\int_{a_0}^{a_i}\frac{da}{(\beta\sqrt{\pi a})^{p_I}}\right] \tag{9}$$

By forming the life ratio (N_i^p/N_f^p) for the lives from a_0 to a_i and a_0 to a_f, the stress effect is eliminated totally when using Eq. (9), i.e.

$$\frac{N_i^p}{N_f^p} = \left[\int_{a_0}^{a_i}\frac{da}{(\beta\sqrt{\pi a})^{p_I}}\right]\Bigg/\left[\int_{a_0}^{a_f}\frac{da}{(\beta\sqrt{\pi a})^{p_I}}\right] \tag{10}$$

However, when using Eq. (7) to develop a similar life ratio, Eq. (11)

$$\frac{N_i^p}{N_f^p} = \frac{\left[\left(\frac{K_c}{\sigma_{max}}\right)\int_{a_0}^{a_i}\frac{da}{(\beta\sqrt{\pi a})^{p}} - \int_{a_0}^{a_i}\frac{da}{(\beta\sqrt{\pi a})^{p-1}}\right]}{\left[\left(\frac{K_c}{\sigma_{max}}\right)\int_{a_0}^{a_f}\frac{da}{(\beta\sqrt{\pi a})^{p}} - \int_{a_0}^{a_f}\frac{da}{(\beta\sqrt{\pi a})^{p-1}}\right]} \tag{11}$$

results, showing an explicit relationship between stress and the life ratio. The next subsection describes the presentation of crack growth data in NCG formats and the evaluation of Eqs. (10) and (11).

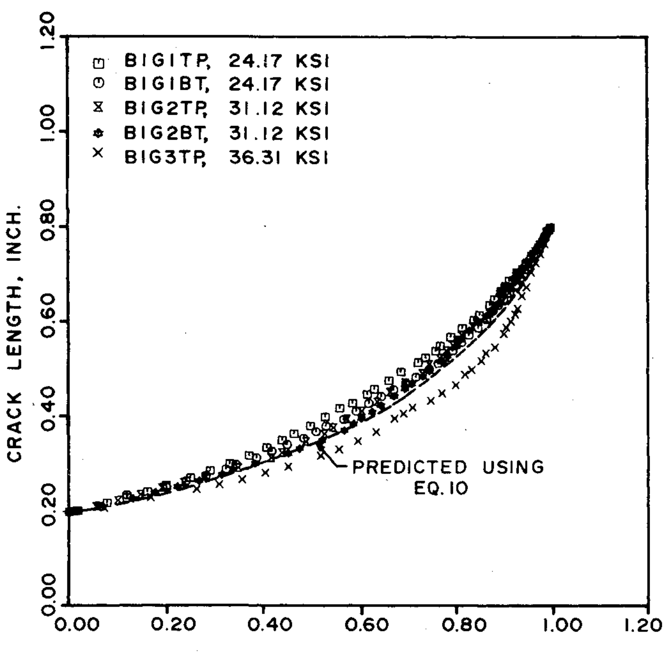

Fig. 9 Type I normalized crack growth data (from Fig. 2) compared to Eq. (10) with $p_I = 3.28$.

Comparison of Experimental and Predicted NCG Curve

To test for stress invariance of the Type I NCG curve [suggested by Eq. (10)], the crack growth data presented in Fig. 2 were life normalized based on initial and final crack lengths of 0.200 and 0.800 in., respectively. This Type I NCG behavior is described by Fig. 9 for five sets of crack growth data; the crack growth set designated BIG3BT was not shown since its final crack length was less than 0.800 in. Also shown in Fig. 9 is a curve derived using Eq. (10) with the exponent $p_I = 3.28$ (see Table 3). The derived curve is seen to represent a mean NCG curve with the data systematically scattered to within ± 10% life ratio bands. Now consider Fig. 10 in which the upper and lower data bands established by the data in Fig. 9 are directly compared to analytical points established by Eq. (11) ($K_c = 70$ ksi $\sqrt{\text{in.}}$, $p = 2.21$). Also shown by Fig. 10, the stress level influence is successfully accounted for by an analysis which more appropriately describes crack growth rate behavior.

The systematic difference between the data and derived [via Eq. (10)] curve in Fig. 9 has an important implication – there is a potential stress influence on the exponent p_I [the exponent p_I in Eq. (10) is the only variable that could be affected by stress level]. A review of Table 2 which lists Eq. (1) least-squares-determined exponents for individual tests confirms that a stress level effect was noted for the given stress history. Based on data in Table 2 for the exponents p_I, one would suspect that the NCG data for the 24.17 and 31.12 ksi maximum stress level conditions would fall close together. Referring to Fig. 9 confirms the suspicion and directs future attention to studies that establish the variance in the exponent p_I which is due to dissimilar load histories. If the variance in the exponent p_I is small, Eq. (10) applies and basic stress invariant hypothesis of the Type I NCG curve can be accepted as reasonable.

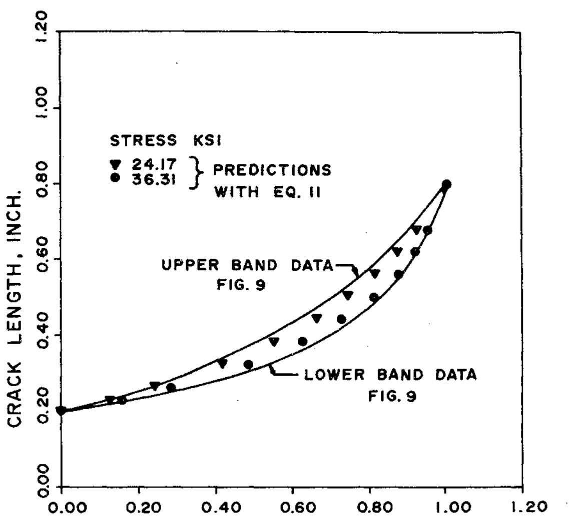

Fig. 10 Type I NCG behavior (from Fig. 9) compared to that predicted from Eq. (11) with $p = 2.21$ and $K_c = 70$ ksi $\sqrt{\text{in}}$.

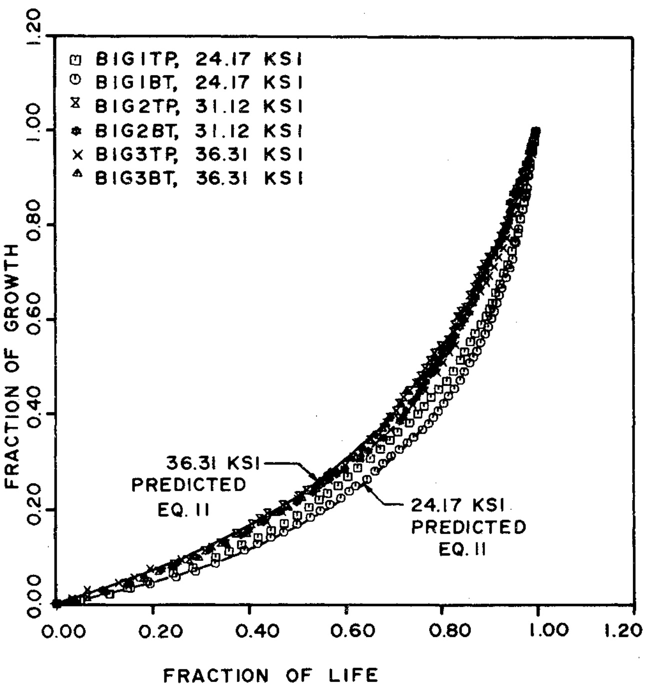

Fig. 11 Type II NCG data compared to that predicted from Eq. (11) with $p = 2.21$, $K_c = 70$ ksi $\sqrt{\text{in}}$., for $a_0 = 0.130$ in. and $a_f = a_{cr}$ from Eq. (12).

As shown by Fig. 10, direct analysis of the observed stress level variation on the Type I curve can be obtained using Eq. (11) to establish the life ratio (N_i^p/N_f^p). This same life ratio equation is also suitably designed for assessing the potential invariance of the Type II NCG curve, where a_f is a_{cr}, a crack length determined by a critical stress versus fracture toughness relationship. For the Type II NCG curve, the final crack length a_{cr} is obtained by inverting Eq. (12),

$$K_{cr} = \sigma_{max} \beta \sqrt{\pi a_{cr}} \tag{12}$$

where K_{cr} can be chosen to be less than or equal to K_c [Eqs. (2), (7), and (11)] and β is appropriately chosen for the geometry of interest. Selecting $a_0 = 0.130$ in. and $K_{cr} = 50$ ksi $\sqrt{\text{in}}$., the center crack growth data in Fig. 2 were converted to the Type II data presented in Fig. 11. Figure 11 also illustrates

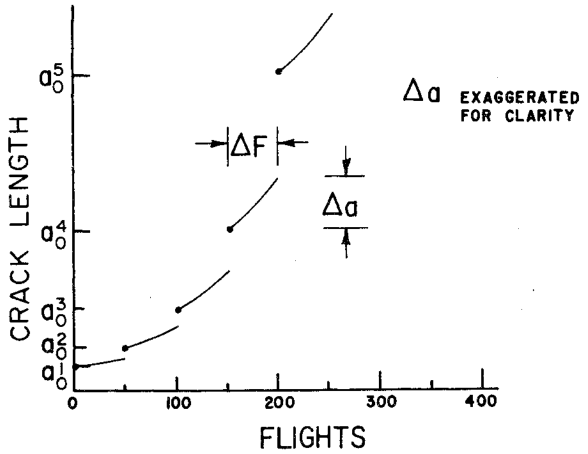

Fig. 12 Simple crack incrementation scheme used to develop crack growth rates analytically.

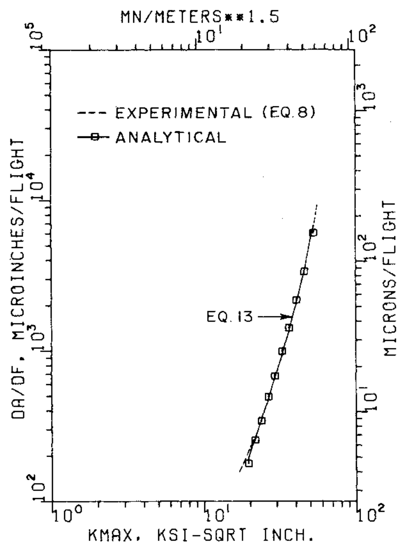

Fig. 13 Crack growth incrementation scheme results compared to equation based on experimental data, i.e. Eq. 8.

that Eq. (11) properly predicts the upper and lower scatter bands for this Type II behavior. By comparing Figs. 9 and 11, it can be seen that the stress effect is reversed. The reason for this Type II NCG curve inversion is due to the differences in final crack length values for the three stress levels. For example, at the $\sigma_{max} = 24.17$ ksi condition, $a_f = 1.135$ in., while at $\sigma_{max} = 36.31$ ksi, $a_f = 0.579$ in. Also note that the scatter in the Type II data is less than that of the Type I data. Further reductions in the Type II data scatter bandwidth can be achieved by decreasing K_{cr} and thus a_f. However, attempts to derive a life ratio equation that would describe the Type II behavior as an invariant geometrical property have not been successful. Nevertheless, utilization of the Type II NCG curve in damage tracking programs can be justified for its ability to condense crack growth data collected under different crack length endpoint conditions.

Developing Crack Growth Rates Analytically

The previous subsection described the interrelationship between crack growth rates and NCG curves, which in turn provided a framework for validating the assumptions used in deriving NCG curves. Furthermore, when crack growth rate equations describe the trend and magnitude of the experimental behavior, the same interrelationship can be used to assess the influences of geometry and stress level on NCG curves and crack growth life. A basic shortcoming of the crack growth rate equation approach is that the experimental data required to establish the curve are costly to collect. The simple crack incrementation scheme presented in Refs. 6 and 11-14 provides the capability for inexpensively developing equations [such as Eqs. (1) or (2)] using analytically established crack growth rate data points.

Figure 12 schematically illustrates the essence of the simple crack incrementation scheme. Crack increments are developed at a series of initial crack lengths by subjecting the chosen geometry to an application of 50 flights. The crack increments are developed using a cycle-by-cycle crack propagation analysis that is responsive to load interaction influences.¶ The 10 Δa increments developed were divided by ΔF (=50 flights) to get the average flight-by-flight crack growth rates shown in Fig. 13 as a function of the stress intensity factor (maximum). Since the purpose in developing these analytical data was to show that they duplicated the experimentally derived behavior as closely as possible, the following was done: 1) a least-squares curve that had the Eq. (2) form with $K_c = 70$ ksi $\sqrt{\text{in.}}$ was fit to these analytical crack growth rate data

$$\frac{\mathrm{d}a}{\mathrm{d}F} = \frac{0.5936 \times 10^{-5} (K_{\max})^{2.489}}{70 - K_{\max}} \tag{13}$$

and, 2) the resulting equation (13) was directly compared to Eq. (8), the equation that was used to describe the experimental data. The resulting analytically developed curve is seen in Fig. 13 to accomplish the desired goals. While not shown here, it can also be demonstrated that the predicted crack growth rate expression [Eq. (13)] leads to NCG curves which closely approximate the NCG data presented in Figs. 9 and 11.

Conclusions

Based on the work presented here and previously,[3,6] we suggest that:

1) The Type I NCG curve can be considered essentially invariant with respect to external inputs (stress history) for a specified geometrical configuration when the variance on the exponent p_l in Eq. (1) is small.

2) The Type II NCG curve can only be considered useful if it successfully collapses crack growth behavior generated under different service stress histories. No analytical justification has yet been suggested to indicate that it is an invariant curve.

3) NCG curves can be established using raw (experimental) crack growth data directly or by inverting crack growth rate equations derived from the crack growth data. The inverted crack growth rate equation technique provides the capability for predicting the influences of geometrical changes or spectrum stress scaling. Steady-state crack growth rate behavior[6] is assumed as a basis for the second technique suggested.

4) If the crack growth rate behavior can be classified as steady-state, then analytical crack incrementation schemes[6,11-14] provide the capability for establishing crack growth rate equations. Since analytical crack growth rate schemes are more cost-effective than collecting the appropriate experimental data, they are suggested for sensitivity studies when evaluating stress and geometrical influences on NCG curves.

¶The analysis employed herein duplicates the procedure and material properties of Ref. 6; only the stress intensity factor coefficient was changed to match the center crack geometry.

References

[1] Coffin, M. D. and Tiffany, C. F., "New Air Force Requirements for Structural Safety, Durability and Life Management," *Journal of Aircraft*, Vol. 13, Feb. 1976, pp. 93-98.

[2] "Airplane Damage Tolerance Requirements," Military Specification, MIL-A-83444 (USAF), July 2, 1974.

[3] Gallagher, J. P. and Bader, R. M., "A Normalized Scheme for Describing Crack Growth Behavior," *Advances in Joining Technology*, edited by J. J. Burke et al., Brook Hill Publishing Company, Chestnut Hill, Mass., 1976, Chap. 21, pp. 515-535.

[4] Clark, W. G. Jr. and Hudak, S. J. Jr., "Variability in Fatigue Crack Growth Rate Testing," *Journal of Testing and Evaluation*, Vol. 3, Nov. 1975, pp. 454-476.

[5] Potter, J. M., "An Experimental and Analytical Study of Spectrum Truncation Effects," Air Force Flight Dynamics Laboratory, Wright-Patterson Air Force Base, AFFDL-TR-73-117, Feb. 1974.

[6] Gallagher, J. P., "Estimating Fatigue Crack Lives for Aircraft: Techniques," *Experimental Mechanics*, Vol. 16, Nov. 1976, pp. 425-433.

[7] Paris, P. C., "The Fracture Mechanics Approach to Fatigue," *Fatigue, An Interdisciplinary Approach*, edited by J. J. Burke, N. L. Reed, and V. Weiss, Syracuse University Press, 1964, pp. 107-132.

[8] Clark, W. G. Jr., "Fracture Mechanics in Fatigue," *Experimental Mechanics*, Vol. 11, Sept. 1971, pp. 421-428.

[9] Pinckert, R. E., "Damage Tolerance Assessment of F-4 Aircraft," AIAA Paper 76-904, presented at AIAA Aircraft Systems and Technology Meeting, Dallas, Texas, Sept. 27-29, 1976.

[10] Rudd, J. L. and Gray, T. D., "Quantification of Fastener Hole Quality," *Proceedings of the 18th AIAA/ASME Structures, Structural Dynamics, and Materials Conference*, Vol. 1, March 1977, pp. 131-137.

[11] Gallagher, J. P. and Stalnaker, H. D., "Methods for Analyzing Fatigue Crack Growth Rate Behavior Associated with Flight by Flight Loading," AIAA Paper 74-367, presented at the 15th AIAA/ASME/SAE Structures, Structural Dynamics, and Materials Conference, Las Vegas, Nev., April 17-19, 1974.

[12] Gallagher, J. P. and Stalnaker, H. D., "Predicting Flight by Flight Fatigue Crack Growth Rates," *Journal of Aircraft*, Vol. 2, Sept. 1975, pp. 649-705.

[13] Gallagher, J. P., Grandt, A. F. Jr., and Crane, R. L., "Tracking Crack Growth Damage at Control Points," *Proceedings of the 18th AIAA/ASME Structures, Structural Dynamics and Materials Conference*, Vol. 1, March 1977, pp. 101-112.

[14] Gallagher, J. P. and Wood, H. A., "Design Approach for Noninspectable Structures," ASCE Preprint 2865, presented at ASCE Spring Convention and Exhibit, Dallas, Texas, April 25-29, 1977.